

Functional-Coefficient Models for Multivariate Time Series in Designed Experiments: with Applications to Brain Signals

Paolo Victor Redondo, Raphaël Huser and Hernando Ombao
King Abdullah University of Science and Technology

Abstract

To study the neurophysiological basis of attention deficit hyperactivity disorder (ADHD), clinicians use electroencephalography (EEG) which record neuronal electrical activity on the cortex. The most commonly-used metric in ADHD is the theta-to-beta spectral power ratio (TBR) that is based on a single-channel analysis. However, initial findings for this measure have not been replicated in other studies. Thus, instead of focusing on single-channel spectral power, a novel model for investigating interactions (dependence) between channels in the entire network is proposed. Although dependence measures such as coherence and partial directed coherence (PDC) are well explored in studying brain connectivity, these measures only capture linear dependence. Moreover, in designed clinical experiments, these dependence measures are observed to vary across subjects even within a homogeneous group. To address these limitations, we propose the mixed-effects functional-coefficient autoregressive (MX-FAR) model which captures between-subject variation by incorporating subject-specific random effects. The advantages of MX-FAR are the following: (1.) it captures potential non-linear dependence between channels; (2.) it is nonparametric and hence flexible and robust to model mis-specification; (3.) it can capture differences between groups when they exist; (4.) it accounts for variation across subjects; (5.) the framework easily incorporates well-known inference methods from mixed-effects models; (6.) it can be generalized to accommodate various covariates and factors. Finally, we apply the proposed MX-FAR model to analyze multichannel EEG signals and report novel findings on altered brain functional networks in ADHD.

Keywords: Attention deficit hyperactivity disorder; Electroencephalogram; Non-linear time series; Mixed-effects models; Multivariate time series.

1 Introduction

Attention deficit/hyperactivity disorder (ADHD) is one of the most common cognitive disorders (Alchalabi et al. 2018) that is mostly prevalent among children (Chen et al. 2019). Individuals with ADHD show symptoms including locomotor hyperactivity (overactive), impulsive behavior, excitability, emotional immaturity, short attention span (inattentive), distractibility, and inefficiency at school or work (Gualtieri & Johnson 2005). Persistence of the disorder until adulthood could lead to poor academic performance and problems in social interactions that may become a lingering concern. In some extreme cases, adult ADHD patients suffer from one or more additional psychiatric disorders on top of mood and anxiety disorders, personality disorders and even substance abuse (Sobanski 2006). Driven by the severity of the impact of this medical condition, the goal in this paper is to develop new statistical models that can be used by clinicians to study alterations in brain function that are associated with ADHD. We develop a formal model under which we can identify differences in brain functional networks between the healthy controls and the ADHD population using EEG data.

Characterization of ADHD remains highly debated as the current descriptors of the disorder is too broad (lacks unique attribution compared to other behavioral and learning disorders) and rely heavily on the reports of behavioral symptoms (Swartwood et al. 2003). To develop more objective measures, many pursue the use of neuroimaging modalities such as functional magnetic resonance imaging (fMRI) (Jiang et al. 2019, Cortese et al. 2012, Brown et al. 2012) and electroencephalography (EEG). The potential utility of EEG in understanding ADHD is vast because it is easy to collect, relatively inexpensive, suitable for naturalistic experiments and has excellent temporal resolution (at the millisecond scale) (Lenartowicz & Loo 2014) which allows one to investigate stimulus-induced changes in brain activity as well as the evolution of the underlying brain process across the entire experiment. The standard approach to analyzing EEGs is to decompose its total variance into the power explained by different frequency bands: delta (0.5–4 Hz), theta (4–8 Hz), alpha (8–12 Hz), beta (13–30 Hz), and gamma (30–100 Hz) (Nunez et al. 2016, Cimenser et al. 2011, Nunez et al. 2006, Ombao et al. 2005). From the very first findings of slow-wave EEG activity in the theta frequency band (Jasper et al. 1938), recent studies explore on the difference in spectral power of the EEG signals from individuals with ADHD and normal

(without any behavioral and learning disorder) controls. One of the most popular metric is the theta-to-beta power ratio (TBR). This is associated with ADHD patients having higher theta power (in the fronto-central brain regions) and lower beta power (temporal regions) compared to healthy controls. However, results from the previous works have not yet been replicated and, for this reason, has not reached benchmark status in the community. For an in-depth meta-analysis and comparison of recent TBR researches, see Arns et al. (2013) and van Dijk et al. (2020).

Although analysis on spectral power offers an objective view to study the neurophysiological basis of mental diseases, its applicability in ADHD is yet to be demonstrated. Thus, a complementary approach to spectral analysis of EEG from a single channel is to examine the cross-dependence between channels in a network. Coherence and partial directed coherence (PDC) are two of the most considered dependence measures in the literature of EEG analysis. Testing for significant differences in the brain connectivity between people with and without cognitive disorder (such as ADHD and dyslexia) based on these measures provided interesting insights (see for example Barry et al. (2002), Tcheslavski & Beex (2006), Murias et al. (2007), Clarke et al. (2007), Erkuş (2017), Muthuraman et al. (2019)). However, these measures capture only linear dependence, and hence, one of the major limitations of these metrics is that they fail to identify nonlinear dependence structure in cross-channel dependence in the brain network. Specifically, in the case where the dynamic dependence between channels is driven by some reference signal, a universal linear measure of dependence becomes inappropriate. In addition, since these dependence measures are not directly observed, they have to be estimated for each individual. This introduces a number of disadvantages including neglecting shared attributes across similar ADHD-type subgroups and requiring homogeneity among subject in term of age, gender, etc. Figure 1 shows two-second EEG recordings from some subjects in different groups and we see that, within groups, some patterns are prominent among all its subjects with individual variations. Hence, the goal is to develop a statistical method that can capture the non-linear interactions between the channels common within a group and address the subject-specific variations in the data.

In this paper, we develop a class of models which accounts for (a.) the non-linear interactions between channels in a brain network through the functional-coefficient autoregressive (FAR) model, thus overcoming the limitations of the classical VAR model as well

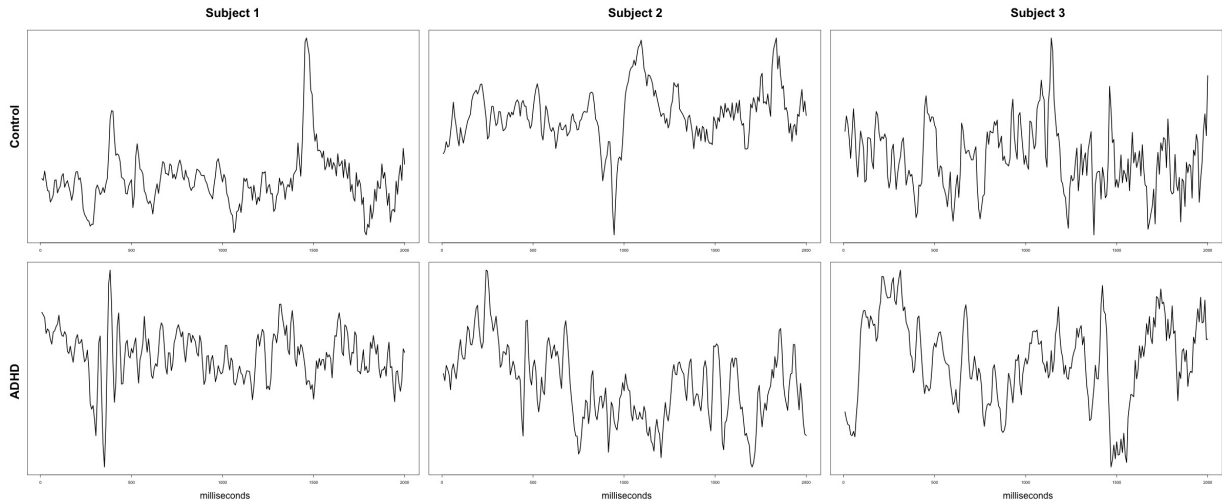


Figure 1: Two-second EEG recordings from channel Fp1 of some subjects in the ADHD and control group.

as coherence and partial directed coherence, and (b.) the variation in brain network across subjects. In Section 5, by considering a reference signal that drives the cross-dependence, we introduce the new concept of functional partial directed coherence, which is directly derived from the autoregressive coefficient functions, congruent with the common PDC calculated from VAR coefficients. This provides a more informative and easy-to-interpret nonlinear measure of dependence. To address the well-known problem of substantial variation between subjects, we propose a mixed-effects modeling framework, which includes subject-specific random effects. This allows us to aggregate information that is common subjects; to derive a collective summary of the temporal dependencies shared through the entire dataset; and it enables subject-specific inference. The remainder of this paper is organized as follows. Section 2 provides the specification of the FAR model in the univariate and multivariate context. Details of the postulated mixed-effects FAR model and the proposed flexible non-parametric estimation method are developed in Section 3. To investigate non-linear cross-dependence between channels in an EEG network, we use the proposed model in Section 5 where we report novel findings and interesting results that identify alterations in brain functional connectivity. Lastly, Section 6 points to future extensions of our work.

2 Functional-Coefficient Autoregressive Model

Denote $Y_{j,t}$ to be the EEG recording at channel j and time t . One of the goals here is to develop a statistical framework for investigating how a *past* observation in channel g might have an impact on *future* observations at channel j (in notation, $X_g(t) \rightarrow X_j(t+L)$), for some time lag L . Given the complexity of brain systems, we express these channel interactions as non-linear functions of some reference signal (defined below). This complex dependence dynamics is captured by the functional-coefficient autoregressive (FAR) model, which we develop in this section.

2.1 Univariate Time Series

A time series $\{Y_t, t = 1, 2, \dots, T\}$ follows a FAR process if it can be represented as

$$Y_t = \sum_{\ell=1}^p f_{\ell}(\mathbf{Y}_{t-1}^*) Y_{t-\ell} + \varepsilon_t, \quad (1)$$

where $p \in \mathbb{Z}^+$, $\{\varepsilon_t\} \sim WN(0, \sigma_{\varepsilon}^2)$ (see Chen & Tsay (1993)). Here, the vector $\mathbf{Y}_{t-1}^* = (Y_{t-\ell_1}, Y_{t-\ell_2}, \dots, Y_{t-\ell_c})'$, where $\ell_l > 0, l = 1, 2, \dots, c$, and $\{\varepsilon_t\}$ is Gaussian white noise with mean zero and variance σ_{ε}^2 . Hence, \mathbf{Y}_{t-1}^* takes on only past values and does not rely on any future outcomes. For the EEG analysis, we refer to \mathbf{Y}_{t-1}^* as the ‘‘reference’’ signals. Moreover, $f_{\ell}(\mathbf{Y}_{t-1}^*)$ ($\ell = 1, 2, \dots, p$) are measurable functions from \mathbb{R}^c to \mathbb{R} , which map all the variables into the real line. That is, the dependency of Y_t on the past measurements $Y_{t-\ell}$ are functions of the observed reference signals. In practice, these functional coefficients $f_{\ell}(\cdot)$ s may include some deterministic sequence (e.g., convolution of sequence of stimulus presentation), recordings from an EEG channel (or a summary from a group of channels), possibly an extraneous physiological signal.

Consider a single reference signal, i.e., $\mathbf{Y}_{t-1}^* = Y_{t-d}$, for some fixed lag d . One special case of FAR is the threshold autoregressive (TAR) model where $f_{\ell}(Y_{t-d}) = \phi_{\ell}^{(1)} I(Y_{t-d} \leq \eta) + \phi_{\ell}^{(2)} I(Y_{t-d} > \eta)$ where $I(\cdot)$ is the usual indicator function and Y_{t-d} is the threshold variable. On the other hand, if $f_{\ell}(Y_{t-d}) = \phi_{\ell}$, that is, the coefficient is independent of Y_{t-d} and is a constant, then, under regularity conditions, the FAR model translates to the Gaussian AR process (Shumway et al. 2000, Brockwell & Davis 2009). In general, the $f_{\ell}(\cdot)$ s can take on various possible forms.

Initially, Chen & Tsay (1993) developed the arranged local regression (ALR) to create plots that facilitate visualization of the empirical form of functional coefficients. From these plots, a parametric model is then proposed and is estimated. However, this often results in a poor fit (or overparameterization) due to the difficulty in specifying parsimonious parametric forms for the coefficients. Hence, nonparametric approaches for estimating the $f_\ell(\cdot)$ s are explored. Cai et al. (2000) and Chen & Liu (2001) both implemented local linear regression, while Huang & Shen (2004) proposed a polynomial splines-based global smoothing approach for estimation. In this paper, we focus on the local linear regression approach as it provides an intuitive way to extend the FAR model to the mixed-effects framework.

For ease of exposition, we adapt the usual notation in linear models, where $\mathbf{Y} = \{Y_t\}$ refers to the response variable and $\mathbf{X}_\ell = \{X_{\ell,t}\} = \{Y_{t-\ell}\}$, $\ell = 1, 2, \dots, p$ are the covariates of lagged responses. Also, we assume only a single reference signal for all functional coefficients, denoted by $\mathbf{U} = \{U_t\}$. Thus, the model is rewritten as follows:

$$Y_t = \sum_{\ell=1}^p f_\ell(U_t)X_{\ell,t} + \varepsilon_t \quad \text{where } \{\varepsilon_t\} \sim WN(0, \sigma_\varepsilon^2). \quad (2)$$

Note that in Equation (2), each $f_\ell(\cdot)$ shares the same reference signal. Now, consider a specific value in the domain of U_t , say u_0 . For all values of U_t in the neighborhood of u_0 (i.e., for all U_t such that $|U_t - u_0| < r$ where the radius $r > 0$), we approximate each $f_\ell(U_t)$ as a local linear function. Specifically, we assume $f_\ell(U_t) \approx \alpha_\ell + \beta_\ell(U_t - u_0)$, for all $\ell = 1, 2, \dots, p$. Hence, we define the local linear estimator as $\hat{f}_\ell(u_0) = \hat{\alpha}_\ell$, where $\{(\hat{\alpha}_\ell, \hat{\beta}_\ell)\}$ minimizes

$$\sum_{t=1}^T \left\{ Y_t - \sum_{\ell=1}^p [\alpha_\ell + \beta_\ell(U_t - u_0)] X_{\ell,t} \right\}^2 K_h(U_t - u_0) \quad (3)$$

where, $K_h(u) = h^{-1}K(u/h)$, with a specified kernel function K , and a fixed bandwidth $h > 0$. Suppose $\hat{\underline{\alpha}} = (\hat{\alpha}_1, \hat{\alpha}_2, \dots, \hat{\alpha}_p)'$, $\hat{\underline{\beta}} = (\hat{\beta}_1, \hat{\beta}_2, \dots, \hat{\beta}_p)'$ and $\hat{\underline{\theta}} = (\hat{\underline{\alpha}}', \hat{\underline{\beta}}')$. The solution to the weighted least squares problem (3) is given by

$$\hat{\underline{\theta}} = \begin{pmatrix} \hat{\underline{\alpha}} \\ \hat{\underline{\beta}} \end{pmatrix} = \left(\tilde{\mathbf{X}}' \mathbf{W} \tilde{\mathbf{X}} \right)^{-1} \tilde{\mathbf{X}}' \mathbf{W} \mathbf{Y}, \quad (4)$$

where $\tilde{\mathbf{X}}$ is a $T \times 2p$ matrix with the t -th row equal to $[\mathbf{X}'_t, \mathbf{X}'_t(U_t - u_0)]$ such that

$\underline{\mathbf{X}}_t' = (X_{1,t}, \dots, X_{p,t})'$ and $\underline{\mathbf{W}} = \text{diag}\{K_h(U_1 - u_0), \dots, K_h(U_T - u_0)\}$.

2.2 Multivariate Time Series

Consider now EEG recordings from k channels and denote the measurements at time t as $\underline{\mathbf{Y}}_t = (Y_{1,t}, \dots, Y_{k,t})'$, which is a k -dimensional vector. Let $\underline{\mathbf{X}}_t = (\underline{\mathbf{Y}}_{t-1}, \dots, \underline{\mathbf{Y}}_{t-p})'$ where $\underline{\mathbf{Y}}_{t-\ell} = (Y_{1,t-\ell}, \dots, Y_{k,t-\ell})$, for all $\ell = 1, 2, \dots, p$, and, assuming only a single reference channel U_t , let $\underline{\mathbf{f}}(U_t) = [\underline{\mathbf{f}}_1(U_t)', \dots, \underline{\mathbf{f}}_k(U_t)']'$ with $\underline{\mathbf{f}}_j(U_t) = [f_{j,1:1}(U_t), \dots, f_{j,k:1}(U_t), \dots, f_{j,1:p}(U_t), \dots, f_{j,k:p}(U_t)]'$, $j = 1, 2, \dots, k$. Note that the j -th row of $\underline{\mathbf{f}}(U_t)$ corresponds to all functional coefficients associated with $Y_{j,t}$. Then, the vector FAR model, as defined by Harvill & Ray (2006), can be written as

$$\underline{\mathbf{Y}}_t = \underline{\mathbf{f}}(U_t)\underline{\mathbf{X}}_t + \underline{\boldsymbol{\varepsilon}}_t, \quad (5)$$

i.e.,

$$\begin{pmatrix} Y_{1,t} \\ Y_{2,t} \\ \vdots \\ Y_{k,t} \end{pmatrix} = \begin{pmatrix} \underline{\mathbf{f}}_1(U_t) \\ \underline{\mathbf{f}}_2(U_t) \\ \vdots \\ \underline{\mathbf{f}}_k(U_t) \end{pmatrix} \underline{\mathbf{X}}_t + \underline{\boldsymbol{\varepsilon}}_t, \quad (6)$$

where $\underline{\boldsymbol{\varepsilon}}_t \sim WN(\mathbf{0}, \sigma_{\boldsymbol{\varepsilon}}^2 \otimes \underline{\mathbf{I}}_k)$. Assuming all $f_{j,g:\ell}(U_t)$, $j, g = 1, 2, \dots, k$, $\ell = 1, 2, \dots, p$, have continuous second-order derivatives, for all U_t in the vicinity of u_0 , each $f_{j,g:\ell}(U_t)$ may be approximated by a local linear function, i.e., $f_{j,g:\ell}(U_t) = \alpha_{j,g:\ell} + \beta_{j,g:\ell}(U_t - u_0)$. Therefore, the estimator for $\underline{\mathbf{f}}(U_t)$, similar to the univariate case, can be obtained by solving a congruent weighted least squares problem. For the detailed discussion, see Harvill & Ray (2006).

3 Mixed-Effects FAR Model

We now generalize the functional-coefficient autoregressive model to the multi-subject mixed-effects framework. Suppose the dataset from a designed experiment consists of EEG recordings from N different subjects. Denote $Y_{j,t}^{(n)}$ to be the EEG recordings at channel j and time t from the n -th subject. The goal now is to capture the functional dynamics in brain networks by characterizing the connection between the past values at channel g and the future recordings from the j -th channel while accounting for subject-specific variations.

By doing so, one can describe channel interactions that are shared across all subjects and provide inference specific to an individual. Hence, we propose a new model which is the mixed-effects functional-coefficient autoregressive (MX-FAR) model. The novel elements and advantages over existing models of the proposed MX-FAR model are stated in the following subsections.

3.1 Univariate Mixed-Effects FAR Model

Consider time series recordings from N subjects, denoted as $Y_t^{(n)}, n = 1, \dots, N$. Then, we define $Y_t^{(n)}$ as an MX-FAR(p) process if, for all $t = 1, 2, \dots, T$,

$$Y_t^{(n)} = \sum_{\ell=1}^p f_{\ell}^{(n)}(U_t^{(n)})X_{\ell,t}^{(n)} + \varepsilon_t^{(n)}, \quad (7)$$

where $f_{\ell}^{(n)}(U_t^{(n)}) = f_{\ell}^{(n)}(U_t^{(n)} | \underline{\lambda}_{\ell}^{(n)})$, $\{\varepsilon_t^{(n)}\} \sim WN(0, \sigma_{\varepsilon}^2)$, and $\varepsilon_t^{(n)}$ is independent of $U_s^{(n)}$ and $X_{\ell,s}^{(n)}$ for all $s < t$. Here, the ℓ -th functional coefficient for the n -th series is now governed by the set of parameters $\underline{\lambda}_{\ell}^{(n)}$. This is one of the advantages of the proposed MX-FAR model. It naturally incorporates the variation across subjects in a flexible manner. For example, $f_{\ell}^{(n)}(U_t^{(n)})$ can take the form $\lambda_1 \exp\{-(\lambda_2 + \lambda_3^{(n)})(U_t^{(n)})^2\}$. The set of parameters is $\{\lambda_1, \lambda_2, \lambda_3^{(n)}\}$ where the first two are common to all subjects in a population while the last parameter is specific only to subject n . As a result, given an observed $U_t^{(n)}$, the subject-specific component is multiplicative. Another example, in threshold AR models, if $f_{\ell}^{(n)}(U_t^{(n)}) = \lambda_1 I(U_t^{(n)} \leq c) + \lambda_2 I(U_t^{(n)} > c) + \lambda_3^{(n)}$, then the subject-specific component becomes additive. Hence, our model accounts for the possibility that the dynamics can change from one subject to another, which is frequently encountered in brain imaging data. Furthermore, Equation (7) is congruent with Equation (2). Specifically, for $N = 1$, i.e., for the single subject case, the proposed model translates back to the original FAR model of Chen & Tsay (1993) and hence, inherits its nice properties.

For simplicity, assume the reference signal to be the same for all $f_{\ell}^{(n)}(U_t^{(n)}), \ell = 1, \dots, p$. Then, similar to the single subject case, for $U_t^{(n)}$ in a small neighborhood around u_0 , we can approximate each $f_{\ell}^{(n)}(U_t^{(n)})$ locally at u_0 by a linear function $f_{\ell}^{(n)}(U_t^{(n)}) \approx \alpha_{\ell}^{(n)} + \beta_{\ell}^{(n)}(U_t^{(n)} - u_0)$, for all $\ell = 1, 2, \dots, p$, where $\alpha_{\ell}^{(n)} = \alpha_{\ell} + a_{\ell}^{(n)}$, $\beta_{\ell}^{(n)} = \beta_{\ell} + b_{\ell}^{(n)}$, and we assume that $\{a_{\ell}^{(n)}, b_{\ell}^{(n)}\}$ are independent for all $\ell = 1, \dots, p$, and $a_{\ell}^{(n)} \sim N(0, \sigma_{\alpha_{\ell}}^2)$ and $b_{\ell}^{(n)} \sim N(0, \sigma_{\beta_{\ell}}^2)$,

for some variances $\sigma_{\alpha_\ell}^2$ and $\sigma_{\beta_\ell}^2$ to be estimated from the data. Thus, we define the local linear estimator as $\hat{f}_\ell^{(n)}(u_0) = \hat{\alpha}_\ell + \hat{a}_\ell^{(n)}$, where $\{(\hat{\alpha}_\ell, \hat{a}_\ell^{(n)}, \hat{\beta}_\ell, \hat{b}_\ell^{(n)})\}$ minimizes

$$\begin{aligned} \sum_{n=1}^N \sum_{t=1}^T \left[Y_t^{(n)} - \sum_{\ell=1}^p \{(\alpha_\ell + a_\ell^{(n)}) + (\beta_\ell + b_\ell^{(n)})(U_t^{(n)} - u_0)\} X_{\ell,t}^{(n)} \right]^2 K_h(U_t^{(n)} - u_0) \quad (8) \\ + \sum_{n=1}^N \sum_{\ell=1}^p \lambda_{\alpha_\ell} (a_\ell^{(n)})^2 + \sum_{n=1}^N \sum_{j=1}^p \lambda_{\beta_\ell} (b_\ell^{(n)})^2, \end{aligned}$$

for some regularization parameters $\lambda_{\alpha_\ell}, \lambda_{\beta_\ell} > 0$.

Note that the objective function (8) suggests estimating the parameters by minimizing the sum of weighted squared residuals while penalizing for the contribution of the random effects $a_\ell^{(n)}$ and $b_\ell^{(n)}$. The tuning parameters λ_{α_ℓ} and λ_{β_ℓ} can be specified through some cross-validation method; however, given the number of subjects N , total data points T and the autoregressive order p , this becomes computationally exhausting. Hence, we provide a conservative penalty instead. For a specific random effect, say $a_\ell^{(n)}$, we assume its contribution to be inversely proportional to its variance $\sigma_{\alpha_\ell}^2$. On the other hand, since the functional coefficients estimated locally at u_0 , the criterion incorporates the weight $K_h(U_t^{(n)} - u_0)$. This becomes conservative by considering $\max\{K_h(U_t^{(n)} - u_0)\}$. Hence, we propose the tuning parameters as $\lambda_{\alpha_\ell} = \lambda \frac{\sigma_{\alpha_\ell}^2}{\max\{K_h(U_t^{(n)} - u_0)\}}$ and $\lambda_{\beta_\ell} = \lambda \frac{\sigma_{\beta_\ell}^2}{\max\{K_h(U_t^{(n)} - u_0)\}}$, that is, a function of a single tuning parameter λ scaled by the variation across subjects and maximum distance from the approximation. In matrix form, (8) can be expressed as

$$[\underline{\mathbf{Y}} - (\underline{\mathbf{X}}\underline{\boldsymbol{\theta}} + \underline{\mathbf{Z}}\underline{\boldsymbol{\gamma}})]' \underline{\mathbf{W}} [\underline{\mathbf{Y}} - (\underline{\mathbf{X}}\underline{\boldsymbol{\theta}} + \underline{\mathbf{Z}}\underline{\boldsymbol{\gamma}})] + \underline{\boldsymbol{\gamma}}' \underline{\mathbf{G}}^{-1} \underline{\boldsymbol{\gamma}} \quad (9)$$

where $\underline{\mathbf{Y}} = (\underline{\mathbf{Y}}^{(1)'}, \dots, \underline{\mathbf{Y}}^{(N)'})'$, $\underline{\mathbf{Y}}^{(n)} = (Y_1^{(n)}, \dots, Y_T^{(n)})'$, $\underline{\mathbf{X}} = (\underline{\tilde{\mathbf{X}}}^{(1)'}, \dots, \underline{\tilde{\mathbf{X}}}^{(N)'})'$, $\underline{\tilde{\mathbf{X}}}^{(n)}$ is a $T \times 2p$ matrix such that its t -th row is equal to $(\underline{\mathbf{X}}_t^{(n)'}, \underline{\mathbf{X}}_t^{(n)'}(U_t^{(n)} - u_0))$ with $\underline{\mathbf{X}}_t^{(n)'}$ = $(X_{1,t}^{(n)}, X_{2,t}^{(n)}, \dots, X_{p,t}^{(n)})'$, $\underline{\mathbf{Z}}$ is a block diagonal matrix of $\underline{\tilde{\mathbf{Z}}}^{(n)} = \underline{\tilde{\mathbf{X}}}^{(n)}$, $\underline{\mathbf{W}}$ is a block diagonal matrix formed by the subject-specific kernel weights $\underline{\mathbf{W}}^{(n)} = \text{diag}\{K_h(U_1^{(n)} - u_0), \dots, K_h(U_T^{(n)} - u_0)\}$, $\underline{\mathbf{G}}^{-1} = \underline{\boldsymbol{\lambda}} \otimes \underline{\mathbf{I}}_N$ with $\underline{\boldsymbol{\lambda}} = \text{diag}\{\lambda_{\alpha_1}, \lambda_{\beta_1}, \dots, \lambda_{\alpha_p}, \lambda_{\beta_p}\}$, $\underline{\boldsymbol{\theta}} = (\underline{\boldsymbol{\alpha}}' \ \underline{\boldsymbol{\beta}})'$ with $\underline{\boldsymbol{\alpha}} = (\alpha_1, \alpha_2, \dots, \alpha_p)'$ and $\underline{\boldsymbol{\beta}} = (\beta_1, \beta_2, \dots, \beta_p)'$, and $\underline{\boldsymbol{\gamma}} = (\underline{\boldsymbol{\gamma}}^{(1)'}, \dots, \underline{\boldsymbol{\gamma}}^{(N)'})'$ with $\underline{\boldsymbol{\gamma}}^{(n)} = (\underline{\mathbf{a}}^{(n)'}, \underline{\mathbf{b}}^{(n)'})'$, $\underline{\mathbf{a}}^{(n)} = (a_1^{(n)}, \dots, a_p^{(n)})'$ and $\underline{\mathbf{b}}^{(n)} = (b_1^{(n)}, \dots, b_p^{(n)})'$.

Now, the expression (9) resembles the objective function minimized by the solution of Henderson's mixed model equations (Henderson 1953). Therefore, the functional coefficient

estimates can be obtained as solutions to

$$\begin{pmatrix} \underline{\mathbf{X}}' \underline{\mathbf{W}} \underline{\mathbf{X}} & \underline{\mathbf{X}}' \underline{\mathbf{W}} \underline{\mathbf{Z}} \\ \underline{\mathbf{Z}}' \underline{\mathbf{W}} \underline{\mathbf{X}} & \underline{\mathbf{Z}}' \underline{\mathbf{W}} \underline{\mathbf{Z}} + \underline{\mathbf{G}}^{-1} \end{pmatrix} \begin{pmatrix} \underline{\boldsymbol{\theta}} \\ \underline{\boldsymbol{\gamma}} \end{pmatrix} = \begin{pmatrix} \underline{\mathbf{X}}' \underline{\mathbf{W}} \underline{\mathbf{Y}} \\ \underline{\mathbf{Z}}' \underline{\mathbf{W}} \underline{\mathbf{Y}} \end{pmatrix} \quad (10)$$

Denote $\widehat{f}_\ell(u_0) = \widehat{\alpha}_\ell$ as the estimated mean functional coefficient while $\widehat{f}_\ell^{(n)}(u_0) = \widehat{\alpha}_\ell + \widehat{a}_\ell^{(n)}$ as the predicted subject-specific functional coefficient. The advantage of our proposed estimation procedure is the extrapolation of the mean behavior of the non-linear dependencies while addressing the variability unique to each subject. In addition, subject-specific inference now becomes possible.

3.2 Multivariate Mixed Effects FAR Model

Consider EEG signals from N subjects recorded at k different channels and denote these as $\underline{\mathbf{Y}}_t^{(n)}, i = 1, \dots, N$ where $\underline{\mathbf{Y}}_t^{(n)} = (Y_{1,t}^{(n)}, Y_{2,t}^{(n)}, \dots, Y_{k,t}^{(n)})'$. Again, $Y_{j,t}^{(n)}$ refers to the EEG recordings at channel j and time t from the n -th subject. We say $\underline{\mathbf{Y}}_t^{(n)}$ follows a vector MX-FAR process of order p if, for all $t = 1, 2, \dots, T$,

$$\underline{\mathbf{Y}}_t^{(n)} = \underline{\mathbf{f}}^{(n)}(U_t^{(n)}) \underline{\mathbf{X}}_t^{(n)} + \underline{\boldsymbol{\varepsilon}}_t^{(n)}. \quad (11)$$

More explicitly, to emphasize channel-specific functional coefficients,

$$\begin{pmatrix} Y_{1,t}^{(n)} \\ Y_{2,t}^{(n)} \\ \vdots \\ Y_{k,t}^{(n)} \end{pmatrix} = \begin{pmatrix} \underline{\mathbf{f}}_1^{(n)}(U_t^{(n)}) \\ \underline{\mathbf{f}}_2^{(n)}(U_t^{(n)}) \\ \vdots \\ \underline{\mathbf{f}}_k^{(n)}(U_t^{(n)}) \end{pmatrix} \underline{\mathbf{X}}_t^{(n)} + \underline{\boldsymbol{\varepsilon}}_t^{(n)}, \quad (12)$$

where $\underline{\mathbf{f}}_j^{(n)}(U_t^{(n)}) = (f_{j,1:1}^{(n)}(U_t^{(n)}), \dots, f_{j,k:1}^{(n)}(U_t^{(n)}), \dots, f_{j,1:p}^{(n)}(U_t^{(n)}), \dots, f_{j,k:p}^{(n)}(U_t^{(n)}))', j = 1, 2, \dots, k$, $\underline{\boldsymbol{\varepsilon}}_t^{(n)}$ is a zero-mean white noise process with variance-covariance matrix $\sigma_\varepsilon^2 \otimes \underline{\mathbf{I}}_k$, and $\underline{\boldsymbol{\varepsilon}}_t^{(n)}$ is independent of $U_s^{(n)}$ and $\underline{\mathbf{X}}_s^{(n)}$ for all $s < t$. Again, for all $j, g = 1, 2, \dots, k$ and $\ell = 1, 2, \dots, p$, assume $f_{j,g:\ell}^{(n)}(U_t^{(n)}) = f_{j,g:\ell}(U_t^{(n)} | \underline{\boldsymbol{\lambda}}_{j,g:\ell}^{(n)})$, i.e., each functional coefficient is governed by a set of parameters with at least one component specific only for the n -th subject.

Note that simultaneously estimating the entire model requires extensive computational

resources. Inclusion of numerous channels (k), larger number of individuals (N) or greater number of timepoints (T) would then require inverting extremely large matrices. To overcome this limitation, our approach is to estimate each component separately. For the j -th channel from $\underline{\mathbf{Y}}_t^{(n)}$, $i = 1, \dots, N$ (in Equation (12)), the functional coefficient will be estimated through the Henderson's mixed model equations (Henderson 1953). The model for the j -th channel is specified to be:

$$Y_{j,t}^{(n)} = \underline{\mathbf{f}}_j^{(n)}(U_t^{(n)}) \underline{\mathbf{X}}_t^{(n)} + \varepsilon_{j,t}^{(n)}. \quad (13)$$

However, there is a caveat to estimating each component separately. Note that Henderson's mixed model equations depend on the penalty matrix $\underline{\mathbf{G}}$ which can vary across components. We denote this as $\underline{\mathbf{G}}_j$. Hence, the estimates of the functional coefficients for the j -th channel $\underline{\mathbf{Y}}_j$, in a small neighborhood u_0 , are derived from the system of equations

$$\begin{pmatrix} \underline{\mathbf{X}}' \underline{\mathbf{W}} \underline{\mathbf{X}} & \underline{\mathbf{X}}' \underline{\mathbf{W}} \underline{\mathbf{Z}} \\ \underline{\mathbf{Z}}' \underline{\mathbf{W}} \underline{\mathbf{X}} & \underline{\mathbf{Z}}' \underline{\mathbf{W}} \underline{\mathbf{Z}} + \underline{\mathbf{G}}_j^{-1} \end{pmatrix} \begin{pmatrix} \underline{\boldsymbol{\theta}} \\ \underline{\boldsymbol{\gamma}} \end{pmatrix} = \begin{pmatrix} \underline{\mathbf{X}}' \underline{\mathbf{W}} \underline{\mathbf{Y}}_j \\ \underline{\mathbf{Z}}' \underline{\mathbf{W}} \underline{\mathbf{Y}}_j \end{pmatrix}. \quad (14)$$

Clearly, from Equation (14), only $\underline{\mathbf{G}}_j^{-1}$ and $\underline{\mathbf{Y}}_j$ differ when estimating the model for each channel which decreases the amount of computations needed.

One advantage of the postulated MX-FAR model is that it offers flexibility as the non-linear dependencies naturally incorporate the subject-specific variations, which can either have an additive or multiplicative effect. Moreover, the proposed estimation method does not require knowledge on the unknown shape or governing parameters of the functional coefficients. The contribution of this paper is that it takes advantage of the local linear estimation approach, and introduces the random effects on the slopes and intercepts of the approximating linear functions. As a result, the estimation can be configured to account for specific features such as having multiple groups, which we explore in Section 5. Hence, the proposed estimation of the MX-FAR model serves as an instrument that can compare the nonlinear interactions among different channels between the ADHD population and healthy controls.

3.3 Bandwidth and Reference Signal Selection

Choosing the appropriate bandwidth is an important aspect of estimating functions via a local linear approximation. A large values of the bandwidth leads to overly smooth estimates of the function (potentially leading to underfitting), while a low bandwidth produces rough estimates (leading to overfitting, i.e., interpolation without summarization). Here, we adapt the modified multi-fold cross-validation method in Cai et al. (2000). Consider two positive integers r and Q such that the number of available time points $T > rQ$. We define Q subseries where the q -th subseries is denoted by $\{\mathbf{Y}_{q,t}^{(n)}, i = 1, 2, \dots, N, t = 1, 2, \dots, T - rq, q = 1, 2, \dots, Q\}$. Using a given subseries $\{\mathbf{Y}_{q,t}^{(n)}\}$, the next steps are to estimate the unknown functional coefficients and calculate the one-step forecasting error for the succeeding r timepoints, i.e., for $t = T - rQ + 1, \dots, T - rQ + r$. Then, the value of the kernel bandwidth h is selected to be the minimizer of the sum of mean squared prediction errors for all subseries. Formally, define $\text{APE}_q(h) = \sum_{n=1}^N \sum_{j=1}^k \sum_{g=1}^k \sum_{t=T-rq+1}^{T-rq+r} (Y_{j,g:t}^{(n)} - \widehat{Y}_{j,g:t|q}^{(n)})^2$, where $q = 1, 2, \dots, Q$. Then the optimal bandwidth h_{opt} is the value of h that minimizes the accumulated prediction error (APE)

$$\text{APE}(h) = \sum_{q=1}^Q \text{APE}_q(h). \quad (15)$$

Here, the one-step ahead predictions $\widehat{Y}_{j,g:t|q}^{(n)}$ are based on functional coefficients computed using the sample $\{(\{\mathbf{Y}_{q,t'}^{(n)}, U_t^{(n)}\}, t' = 1, \dots, T - rq, t = T - rq + 1, \dots, T - rq + r)\}$ with bandwidth $h[T/(T - rq)]^{1/5}$. Note that the contribution of the bandwidth in the estimation of coefficients in each subseries varies depending on the length of the subseries. Similar to Harvill & Ray (2006), we impose the same univariate reference signal across components and use $r = \lfloor 0.1T \rfloor$ and $Q = 4$ as suggested by Cai et al. (2000) throughout our application.

On the other hand, since this is a data-driven method, it can also be used as a guide to select the optimal order p of the MX-FAR model, and also the “best” reference signal U_t (whether a lag value of the series or some exogenous variable) if no to little information about the process being modeled exists. However, if prior knowledge is available (e.g., neurophysiology), then it should be considered to complement the selection suggested by the APE criterion.

3.4 Bootstrap-based Nonlinearity Test

Let $\{\underline{\mathbf{Y}}_t^{(n)}\}$ be a vector of EEG recordings from k channels that follows an MX-FAR(p) process. If its functional coefficients do not depend on any reference signal, i.e., $\underline{\mathbf{f}}^{(n)}(U_t^{(n)}) = \underline{\boldsymbol{\eta}}^{(n)}$, where $\underline{\boldsymbol{\eta}}^{(n)}$ is a matrix of constants independent of $U_t^{(n)}$, then the model reduces to a mixed-effects vector autoregressive (VAR) model (Gorrostieta et al. 2012). This implies linear dependence between channels (conditional on past data, the conditional mean vector is a linear function of past values). To test for the non-linearity of the functional coefficients, consider testing

$$H_0 : \underline{\mathbf{f}}^{(n)}(U_t^{(n)}) = \underline{\boldsymbol{\eta}}^{(n)} \quad \text{vs.} \quad H_1 : \underline{\mathbf{f}}^{(n)}(U_t^{(n)}) \neq \underline{\boldsymbol{\eta}}^{(n)}. \quad (16)$$

Under the null hypothesis H_0 , given an estimator of $\underline{\boldsymbol{\eta}}^{(n)}$, denoted by $\widehat{\underline{\boldsymbol{\eta}}}^{(n)}$, the residual sum of squares RSS is defined as

$$\text{RSS}_0 = \sum_{n=1}^N \sum_{t=1}^T (\underline{\mathbf{Y}}_t^{(n)} - \widehat{\underline{\boldsymbol{\eta}}}^{(n)} \underline{\mathbf{X}}_t^{(n)})^2, \quad (17)$$

while fitting an MX-FAR model produces the sum of squared residuals

$$\text{RSS}_1 = \sum_{n=1}^N \sum_{t=1}^T \{\underline{\mathbf{Y}}_t^{(n)} - \underline{\mathbf{f}}^{(n)}(U_t^{(n)}) \underline{\mathbf{X}}_t^{(n)}\}^2. \quad (18)$$

Then, the test statistic is given by $L = \text{RSS}_0 / \text{RSS}_1 - 1$. A large value of L is an indication of evidence against the null hypothesis of linearity where rejection of the null hypothesis is based on large values of L . To avoid assuming an exact reference distribution for L , we develop a new bootstrap procedure in the mixed-effects setting, congruent to Cai et al. (2000). The outline of the procedure is provided below:

1. Estimate an MX-FAR(p) model for the observed data and define the collection of subject-specific centered residuals $\{\underline{\mathbf{r}}_t^{(n)} - \bar{\underline{\mathbf{r}}}^{(n)}\}$ where $\bar{\underline{\mathbf{r}}}^{(n)}$ is the k -dimensional mean vector of the model residuals, i.e., $\bar{\underline{\mathbf{r}}}^{(n)} = \frac{1}{T-p} \sum_{t=p+1}^T r_{j,t}$, $j = 1, \dots, k$, where $\underline{\mathbf{r}}_t^{(n)} = \underline{\mathbf{Y}}_t^{(n)} - \underline{\mathbf{f}}^{(n)}(U_t^{(n)}) \underline{\mathbf{X}}_t^{(n)}$, $t = p+1, \dots, T$.
2. Sample bootstrap residuals from the collection of centered residuals and construct

the bootstrap sample

$$\underline{\mathbf{Y}}_t^{(n),b} = \hat{\underline{\boldsymbol{\eta}}}^{(n)} \underline{\mathbf{X}}_t^{(n)} + \underline{\mathbf{r}}_t^{(n),b}.$$

3. Compute the test statistic L^b by replacing the observed data $\underline{\mathbf{Y}}_t^{(n)}$ with the bootstrap sample $\underline{\mathbf{Y}}_t^{(n),b}$ in (17) and (18).
4. Calculate the p -value of the test as the relative frequency of the event $\{L^b \geq L\}$ among all bootstrap replicates considered ($b = 1, \dots, B$).
5. Given a specified level of significance $\alpha \in (0, 1)$, reject the null hypothesis if the p -value is less than α . Otherwise, do not reject H_0 .

Note that, rejecting the null hypothesis indicates nonlinear dependence among components of the vector time series. In the analysis of EEGs, this suggests significance of the impact of the chosen reference signal in the cross-channel interactions. Hence, a more general dependence measure for brain connectivity should be explored instead of the existing measures that only capture linear dependence.

3.5 Computational Considerations and Limitations

The task here is to characterize network dependence in a k -dimensional vector time series from N subjects through an MX-FAR(p) model. For any given u_0 in the support of a chosen reference signal, estimation of the corresponding functional coefficients $\underline{\mathbf{f}}_j^{(n)}(u_0)$, $j = 1, 2, \dots, k$, requires manipulation of Henderson's mixed model equations. Specifically, the naive way of calculating the solution involves inverting a $2kp(N+1) \times 2kp(N+1)$ matrix. Obviously, the computational resources needed to accomplish this task grows exponentially with the dimension of the vector time series k , the number of lags p considered and the number of individual series N . A more efficient way to calculate the solution is to use the general formula for matrix inversion in block form. As a result, we can translate the large matrix inversion problem into simply inverting multiple $2kp \times 2kp$ matrices instead. Hence, we transform the computational requirement as a linear function of N . However, the computing time is still an exponential function of k . With this, we limit our application to the EEG dataset by considering only seven channels. The selection of EEG channels is discussed in Section 5.

On the other hand, prediction at a specific time t is calculated given the actual value of the reference signal. For example, if the chosen reference signal is $Y_{j,t-d}$, computing the model residuals needs estimating the coefficients at all observed distinct values of $Y_{j,t-d}$. This is computationally expensive. Hence, we suggest simply segmenting the support of the reference signal into M equal-length intervals and estimating only at discretized representative points. It implies that for an actual value of the reference signal, we find the segment it belongs to and approximate its coefficients using the representative estimate for that interval. Suppose we choose to form $M = 50$ non-overlapping intervals, this reduces the number of times we need to estimate the coefficients from $N \times T$ (assuming all values are distinct) to only $M = 50$ times.

4 Numerical Experiments

In this section, we explore the flexibility of the vector MX-FAR model and investigate the performance of our proposed inference approach through simulations. More precisely, the simulated scenarios highlight the capability of the model in capturing the true mean functional coefficients and predicting the subject-specific coefficient curves. We simulated $N = 10$ bivariate series from an MX-FAR process of order $p = 1$ where each series is of length $T = 500$. Assuming all series come from the same group, the true form of the functional coefficients are shown below.

$$\begin{pmatrix} Y_{1,t}^{(n)} \\ Y_{2,t}^{(n)} \end{pmatrix} = \begin{pmatrix} -0.3 & 0.6e^{-(0.30+\lambda_1^{(n)})(Y_{2,t-2}^{(n)})^2} \\ -0.2 & 0.6e^{-(0.15+\lambda_2^{(n)})(Y_{2,t-2}^{(n)})^2} \end{pmatrix} \begin{pmatrix} Y_{1,t-1}^{(n)} \\ Y_{2,t-1}^{(n)} \end{pmatrix} + \begin{pmatrix} \varepsilon_{1,t}^{(n)} \\ \varepsilon_{2,t}^{(n)} \end{pmatrix}$$

where $\varepsilon_{1,t}^{(n)}, \varepsilon_{2,t}^{(n)} \sim N(0, 1)$, $\lambda_1^{(n)}, \lambda_2^{(n)} \sim N(0, 0.03^2)$, $t = 1, \dots, T$, $n = 1, \dots, N$. We applied our proposed inference procedure, and Figure 2 shows the actual and estimated mean functional coefficients, and the (pointwise) average squared difference between the predicted and true subject-specific coefficient curves. Note that the method captures the true behavior of the nonlinear dependencies while accounting for the added variations present in each series. Predictions for the subject-specific coefficients are closer to the true values as compared to estimating each series independently. Hence, the proposed local linear estimation with random effects not only effectively characterizes the mean dependency features in the data, but also enhances the inference for each individual series.

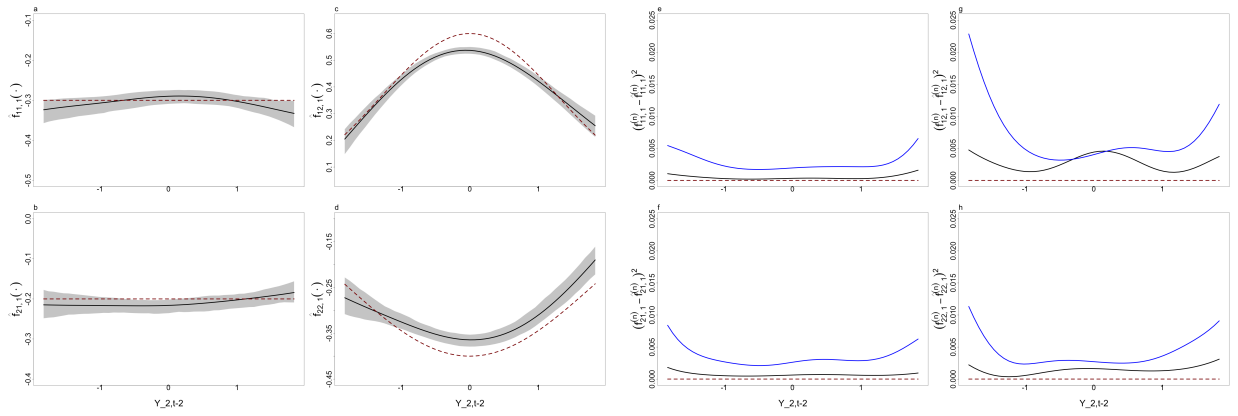


Figure 2: Estimates and average prediction errors for a bivariate MX-FAR($p = 1$) model with EXPAR functional coefficients. Note that a , b , c and d represent the estimates for $f_{1,1:1}(\cdot)$, $f_{1,2:1}(\cdot)$, $f_{2,1:1}(\cdot)$ and $f_{2,2:1}(\cdot)$, respectively, while e , f , g and h present the (pointwise) average squared error of the predicted subject-specific coefficients based on the MX-FAR procedure (black) and on the independent individual estimates (blue).

It is also possible to adapt our modeling framework to account for multiple groups among the series. To illustrate this, we consider another setting, where the same mean (local) slope and intercept coefficients are assumed for series in the same group, while incorporating random effects. We simulated $N = 20$ bivariate series of length $T = 500$ from an MX-FAR process of order $p = 1$ where two groups of the same size are observed. The parametric form of the functional coefficients is provided below. For simplicity, we simulated $N_1 = 10$ series for the first group with the following model:

$$\begin{pmatrix} Y_{1,t}^{(n)} \\ Y_{2,t}^{(n)} \end{pmatrix} = \begin{pmatrix} 0.8 \frac{e^{5Y_{2,t-2}^{(n)}}}{1+e^{5Y_{2,t-2}^{(n)}}} - 0.3 + \lambda_1^{(n)} & 0.2 \\ -0.9 \frac{e^{5Y_{2,t-2}^{(n)}}}{1+e^{5Y_{2,t-2}^{(n)}}} + 0.5 + \lambda_2^{(n)} & 0.3 \end{pmatrix} \begin{pmatrix} Y_{1,t-1}^{(n)} \\ Y_{2,t-1}^{(n)} \end{pmatrix} + \begin{pmatrix} \varepsilon_{1,t}^{(n)} \\ \varepsilon_{2,t}^{(n)} \end{pmatrix}$$

where $\varepsilon_{1,t}^{(n)}, \varepsilon_{2,t}^{(n)} \sim N(0, 1)$, $\lambda_1^{(n)}, \lambda_2^{(n)} \sim N(0, 0.8^2)$, $t = 1, \dots, T$, $n = 1, \dots, N_1$.

As for the second group (comprising $N_2 = 10$ time series), we simply set their coefficients to be the negative of the first group's coefficients. Even though the groups differ greatly, as the functions have opposite behaviors, this does not prevent the proposed estimation to perform well. Figure 3 compares the mean coefficient estimates for the two groups. Note that our method simultaneously estimates the mean functional coefficients of each group, and in this case, is able to mimic the actual group structures.

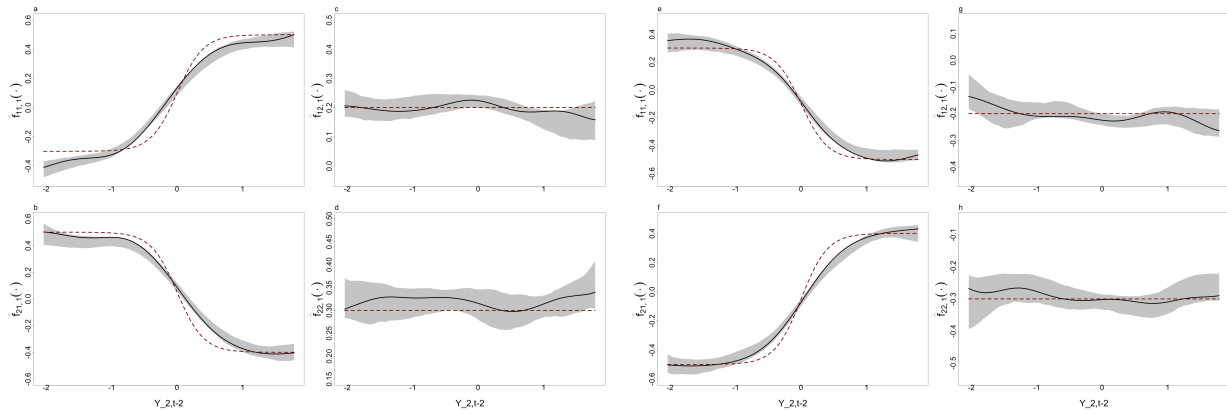


Figure 3: Mean estimates of a bivariate MX-FAR($p = 1$) model with sinusoidal coefficient functions of the first ($a - d$) and second ($e - h$) group. The shaded regions correspond to the 95% bootstrap (pointwise) confidence interval. Note that (a, e) , (b, f) , (c, g) and (d, h) represent the group estimates for $f_{1,1:1}(\cdot)$, $f_{1,2:1}(\cdot)$, $f_{2,1:1}(\cdot)$ and $f_{2,2:1}(\cdot)$, respectively.

5 EEG Analysis: Exploring Non-Linear Dependence in ADHD

Now, we use the MX-FAR model to investigate alterations in brain connectivity among children diagnosed with ADHD, in comparison to children in a healthy control group. There are many challenges to analyzing EEG signals in a designed experiment. First, EEGs are realizations of a highly complex underlying brain functional process. The problem is that most standard time series models are unable to capture non-linear cross-channel interactions in a functional brain network. Second, there is often a significant variation in the brain functional networks across subjects in a population. Thus, to conduct statistical inference brain network connectivity on these populations that is robust to the subject-specific variations, it is essential to utilize information from multiple subjects and derive a "common" functional network that captures the non-linear dependencies. A usual strategy is to perform independent analysis per subject and aggregate the subject-specific estimates using some summary measure (e.g., sample mean). However, this does not fully account for the uncertainty of the subject-specific estimates, which assumes equal contribution from each estimates. Hence, it becomes prone to failure as it does not address presence of unusual subjects, even more so in the context of non-linear multivariate time series analysis.

The novel MX-FAR model is specifically tailored to address these issues. The EEG data (reported in Motie Nasrabadi et al. (2020)) contains scalp EEGs sampled at 128Hz

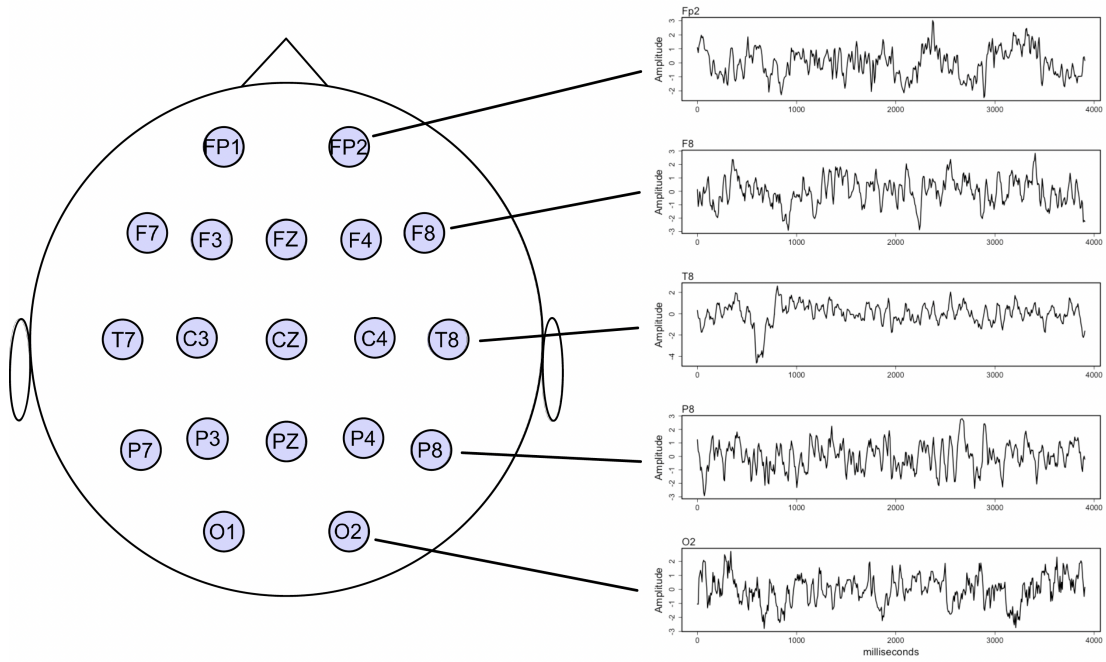


Figure 4: Standard 10-20 EEG scalp topography and a 4-second time window of standardized EEG signals from several channels of a subject with ADHD.

from 19 channels in a cognitive experiment with 104 participants: 51 children diagnosed with ADHD and of a control group of 53 children with no registered psychiatric disorder. Note that the original data has 120 subjects but some EEGs had to be discarded because of severe artifacts and noise that could not be corrected. Pre-processing was conducted via the PREP pipeline of Bigdely-Shamlo et al. (2015) to standardize the EEGs and increase the quality of the recordings. In addition, these EEGs were standardized to a zero-mean unit variance series to transform all observations to a unified scale. Figure 4 shows the standard 10-20 EEG scalp topography and a 4-second time window of standardized EEG signals from several channels of a subject with ADHD.

The visual-cognitive task in the experiment was to count the number of characters after being shown pictures of cartoon characters (see Figure 5). Seven EEG channels of interest were selected that are known to be engaged in this specific process, namely, Fp1 (left pre-frontal), Fp2 (right pre-frontal), O1 (left occipital), O2 (right occipital), T7 (left temporal), T8 (right temporal) and Cz (central), to "represent" brain regions that are most likely engaged for this specific visual-cognitive task. The frontal region is linked with concentration, focus and problem solving, the occipital region for visual processing, and the temporal region for speech and memory (Björge & Emaus 2017). On the other hand,

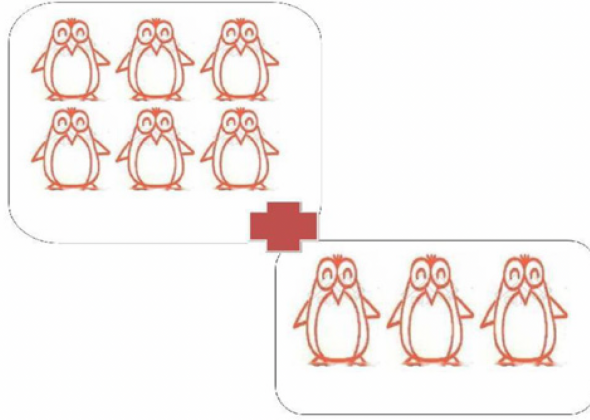


Figure 5: A picture shown to children participants during the experiment (Mohammadi et al. 2016).

the central region is assumed to have a general function and hence, it captures activity over a broad region of the cortex. Here, we investigate the nonlinear cross-dependence patterns in the brain network defined by these selected channels.

To determine the best lag order of the EEGs and the reference signal in the MX-FAR model, the extended APE criterion was employed. This step selects the lag order with the lowest APE while remaining interpretable and yielding significant nonlinear dependence. The best order for MX-FAR process is $p = 4$ with the central channel Cz (at lag 10) as the reference signal. In addition to having produced the smallest APE, channel Cz, which is assumed to be involved in most brain functions, is an intuitive choice for the reference signal that drives the non-linear dependence between other channels.

The electroencephalograms were preprocessed, prior to statistical analysis, according to standard pipelines including artifact removal and bandpass filtering (0.5 - 100 Hertz). Then, they were mean-shifted and rescaled to unit variance. We summarize the non-linear dependence characterized by the MX-FAR model by adapting the concept of partial directed coherence (PDC), originally developed by Baccalá & Sameshima (2001). This concept is further developed here to handle non-linearity in the cross-dependence structure. This dependence measure is calculated based on the Fourier transform of the coefficients of the underlying vector autoregressive (VAR) model and measures the intensity and direction of information flow from one channel to another at a specific frequency. By viewing the MX-FAR process as a VAR process conditional on the observed reference signal, we now define a congruent measure: the *functional partial directed coherence (fPDC)*.

Consider a k -dimensional vector MX-FAR process with lag order p . For a given value u_0 of the reference signal, the f PDC measure is estimated by $\widehat{\mathbf{Y}}^{(n)}(t) = \sum_{\ell=1}^p \widehat{\mathbf{f}}_{\ell}^{(n)}(u_0) \mathbf{Y}^{(n)}(t - \ell)$. For each estimated coefficient function $\widehat{f}_{j,g;\ell}^{(n)}(u_0)$, define

$$\widetilde{f}_{j,g}^{(n)}(\omega, u_0) = \begin{cases} 1 - \sum_{\ell=1}^p \widehat{f}_{j,g;\ell}^{(n)}(u_0) e^{\{-i2\pi\omega\ell\}} & \text{if } j = g \\ - \sum_{\ell=1}^p \widehat{f}_{j,g;\ell}^{(n)}(u_0) e^{\{-i2\pi\omega\ell\}} & \text{otherwise.} \end{cases} \quad (19)$$

Then, the f PDC at frequency ω , given a reference signal value u_0 , from channel g to j is calculated as

$$fPDC_{j,g}^{(n)}(\omega, u_0) = \frac{\widetilde{f}_{j,g}^{(n)}(\omega, u_0)}{\sqrt{\sum_{j^*=1}^k \left| \widetilde{f}_{j^*,g}^{(n)}(\omega, u_0) \right|^2}} \quad (20)$$

Since, by definition, the f PDC is completely analogous to the PDC of Baccalá & Sameshima (2001), the f PDC inherits the nice properties of the original PDC, e.g., its modulus, $|fPDC_{j,g}^{(n)}(\omega, u_0)|$, also takes on values in $[0, 1]$. In addition, by translating the functional coefficients $\widehat{f}_{j,g;\ell}^{(n)}(u_0)$ to $fPDC_{j,g}^{(n)}(\omega, u_0)$, we quantify the intensity and direction of information flow across channel g to j at specific frequency ω , given a certain level u_0 of the reference signal. This now provides more insights as it inherits the non-linearity of the MX-FAR model and gains the interpretation of the original PDC. Moreover, the mean f PDC, shared among the subjects, can easily be calculated from the MX-FAR model. Given the estimated mean functional coefficients $\widehat{\mathbf{f}}_{\ell}(\cdot)$, $\ell = 1, \dots, p$, we define the average information flow from channel g to j as the $fPDC_{j,g}$ derived from $\widehat{\mathbf{f}}_{\ell}(\cdot)$. As a result, this measure provides a characterization of the non-linear interactions within the population while accounting for the subject-specific variations. Note that the defined mean $fPDC_{j,g}$ is not equivalent to the average of $fPDC_{j,g}^{(n)}$, $n = 1, \dots, N$. Using the latter, instead of the proposed measure, leads to incorrect estimates of the intensity of dependence in the brain network. Thus, our MX-FAR model, from which the mean f PDC is obtained, provides better utilization of the data coming from multiple subjects.

An advantage of our proposed MX-FAR model is that, based on the calculated mean f PDC, a common graphical structure for the inter-channel dependencies can be inferred. This non-linear structure (conditional on the value of the reference signal) is shared across all subjects in the population and indicates if the information flow from one channel to

another is significant. More formally, we say that there is a directional interaction from channel g to channel j if, for some $\omega \in (0, 0.5)$, $|fPDC_{j,g}(\omega, u_0)|$ is “large”. To control for false detection, we develop a new threshold inspired by Schelter et al. (2006). Specifically, a significant information flow from channel g to channel j exists, if the estimated 95% bootstrap confidence interval for $|fPDC_{j,g}(\omega, u_0)|$ strictly exceeds the non-linear 0.05-significance level threshold for some frequency ω (see Supplementary Material for the exact form and derivation of the threshold). With this, we can construct a non-linear graphical structure for the brain network of children with and without ADHD and differentiate the inter-channel connectivity between them.

Due to space limitations, it is not possible to report all estimated functional PDCs, but rather summarize the novel findings here as well as provide some plots that justify these points. All remaining plots are reported in the Supplementary Material. Figure 6 shows some of the estimated mean $fPDC$ of the two groups for all frequencies given small and large amplitude of the reference signal. For both the ADHD and control group, the $fPDC$ s related to the flow of information from past values of a channel to itself are close to 1 for all frequencies regardless of the amplitude (both low amplitude and high amplitude) of the reference signal (see Figure 6a). This indicates that there is a strong auto-dependence across all channels that is shared by both the healthy control and ADHD populations. Meanwhile, as shown in Figure 6b, the estimated information flow from channel interactions exhibit varying patterns for different channel pairs. For example, the estimated $fPDC$ from channels Fp2 to Fp1 has greater intensity in the lower frequencies than the higher frequencies for the two groups regardless of the amplitude of the reference signal. On the other hand, the directional link from channel O2 \rightarrow Fp1 is significant at any given amplitude of the reference channel Cz for the control group, while for the ADHD group, it is only significant when the amplitude of the reference is large (see Figure 6c). Additionally, in Figure 6d, there is no significant information flow from channel O1 to Fp2 for the ADHD subjects while significant $fPDC$ is observed for the control group, but only at large amplitudes of Cz. Interestingly, these dynamic differences in channel interactions are hidden unless we consider a reference signal that drives the cross-dependence in the brain network.

The novelty of the proposed MX-FAR model and the non-linear dependence measure $fPDC$ is capturing both linear and non-linear dependence between channels. Figure 7

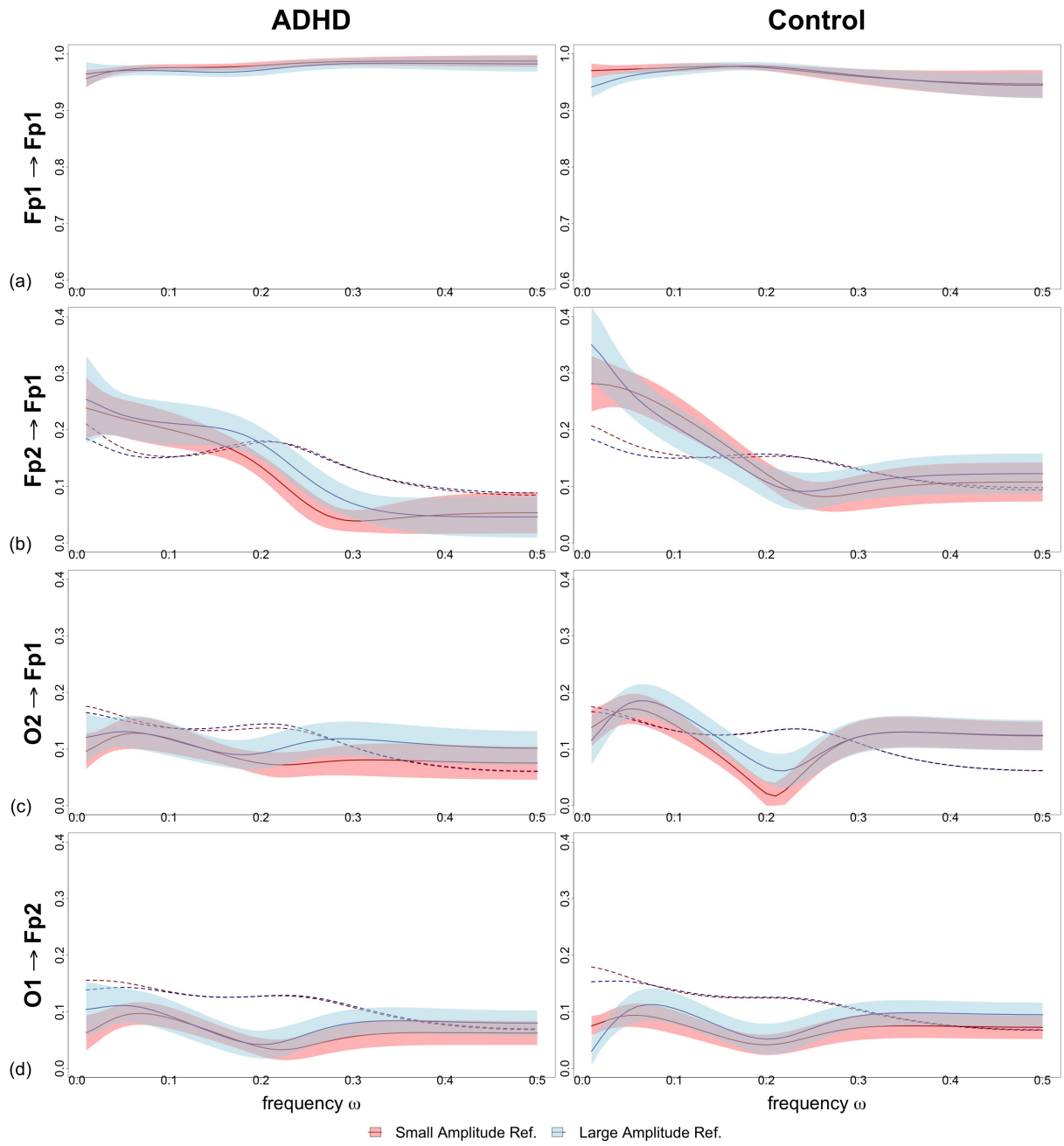


Figure 6: Group mean $fPDC$ estimates for the information flow of one channel to another for all frequencies $\omega \in (0, 0.5)$ given small or large amplitudes of the reference signal (Cz at lag 10). The shaded regions represent the 95% bootstrap confidence interval based on $B = 200$ resamples while the dashed lines are the 0.05-significance level threshold.

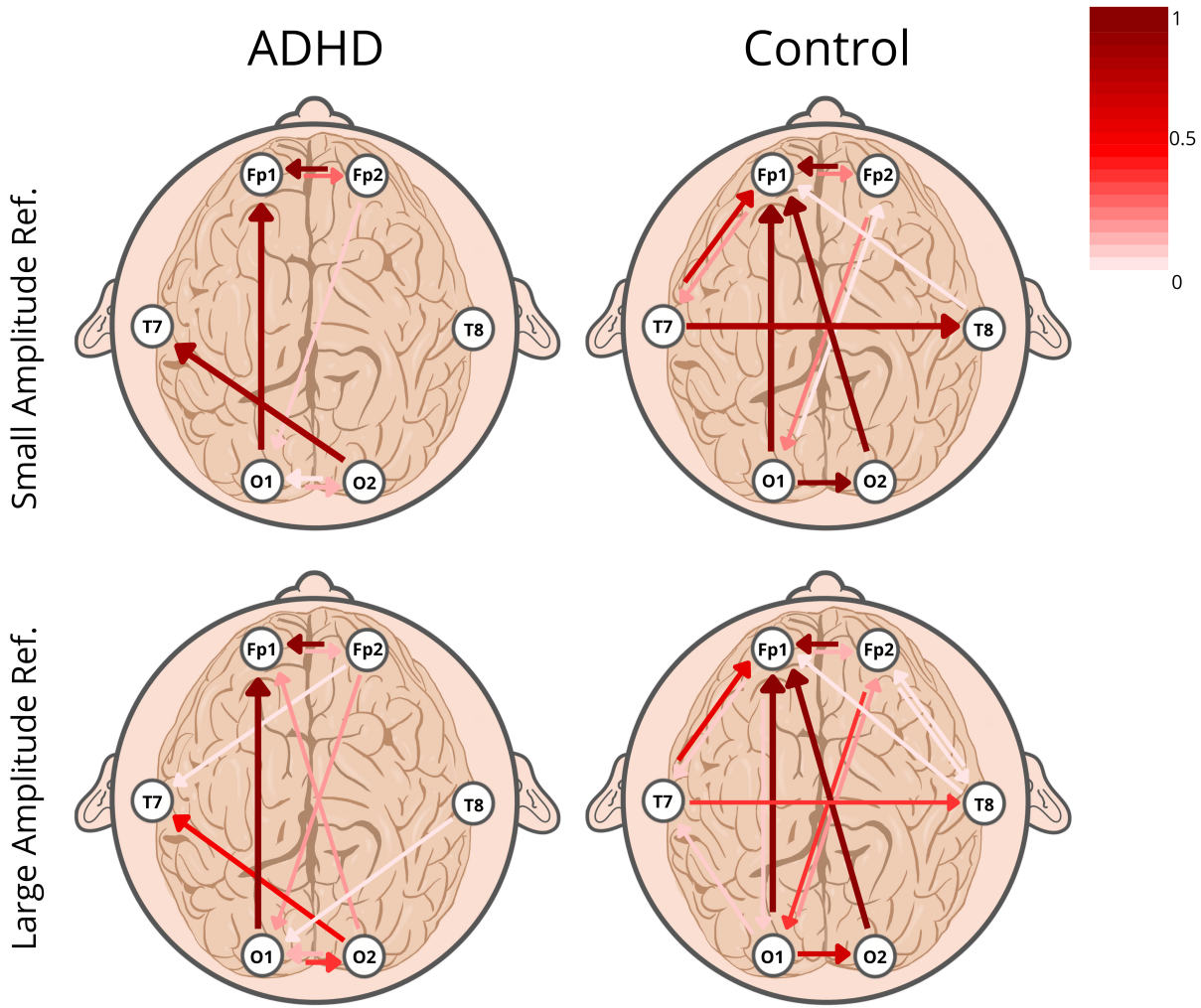


Figure 7: Estimated EEG network of the ADHD and the control group given a small or a large amplitude of the reference signal from the 5-second time window starting at the 10th second.

shows the estimated graphical structures that summarize the cross-dependence between channels of the ADHD and control group across all considered 5-second time windows for small and large amplitude of the reference signal. Darker lines represent higher proportion of time windows where the directional dependence is significant, i.e., an indication of more consistent interaction between two channels throughout the experiment. For subjects with ADHD, we see three relatively consistent inter-channel links, namely, $Fp2 \rightarrow Fp1$; $O1 \rightarrow Fp1$ and $O2 \rightarrow T7$, regardless of the reference signal’s amplitude. Given the cognitive functions to which these channels are associated (pre-frontal to problem solving, temporal to memory and occipital to visual processing), we assume that these direction of information flow is the minimum requirement for ADHD subjects to accomplish the visual task. Moreover, links from $Fp2 \rightarrow O1$ and interaction between the two occipital channels becomes more consistent for large amplitude of the reference signal. Similarly, the directional flow of information from $Fp2 \rightarrow T7$ and from $T8 \rightarrow O1$ only appear during large amplitudes of the reference signal. This is a possible indication that large amplitudes in channel Cz drive more dependence across channels in the non-linear brain network of the ADHD population. We speculate that this might be due to the shorter attention span of ADHD individuals, hence, there is a need to subconsciously remind themselves about the task during the experiment resulting to an “on-off” interaction between channels. Such varying inter-channel connectivity can not be captured if only the usual VAR model and PDC are considered, and hence, our novel MX-FAR model (from which the $fPDCs$ are derived) can indeed capture complex dependency patterns that are prevalent in ADHD patients.

On the other hand, the brain connectivity among healthy controls does not greatly differ with respect to the signal amplitudes at channel Cz. Except for some occasional significant links from $O1 \rightarrow T7$ and interaction between $Fp2 \rightarrow T8$ given large amplitudes of the reference signal, the consistent inter-channel interactions in the brain network of the control group remains throughout the experiment. This points to the linearity of the cross-channel dependence among subjects without ADHD. Instead of having directional links that become significant only when large amplitudes happen in the reference channel Cz (which is evident in the ADHD group), the consistent connectivity patterns among the healthy controls are the same for small and large amplitude signals from Cz. Hence, even though we developed the MX-FAR model to capture non-linear dependence structures, it does not force non-linearity and allows for inference on linear interactions as well.

In general, the (non-ADHD) control group has more prominent brain connectivity network for the associated visual task, compared to the ADHD group. In terms of visual processing, subjects without ADHD optimize information coming from the two occipital channels, unlike subjects in the ADHD group with network links only from one occipital channel O1. Furthermore, channels associated with the same cognitive functions have more consistent directional dependence in the control group, i.e., information flow from Fp2 \rightarrow Fp1, from T7 \rightarrow T8 and from O1 \rightarrow O2 often, if not always, exhibit significant intensities. All these translate to the efficiency in the brain functional network during cognitive processing of healthy control individuals as their brain regions associated with concentration, memory and visual processing function in synchrony during the experiment.

6 Conclusion

Current methods have not been able to extract a universally accepted metric to differentiate young children diagnosed with ADHD from the control population. One limitation of the common techniques for EEG analysis is that they can capture only linear dependence and hence do not account for the complex interactions in the brain network. Moreover, these methods do not properly utilize information from multiple subjects while capturing non-linear interactions. The proposed novel MX-FAR model overcomes these limitations.

One of the advantages of the MX-FAR model is its flexibility: functional coefficients can take either additive or multiplicative subject-specific effects. Furthermore, the proposed estimation approach does not require knowledge of the true functional form of the coefficients nor its governing parameters. Instead, the functions are estimated by assuming a locally linear structure with random effects. Hence, inference method provides good estimates of the true mean functions and account for between-subject variation - even in the presence of abrupt jumps. Moreover, the model can also accommodate for various group-specific features which add another layer of flexibility to the model and hence useful for differentiating the brain functional connectivity networks of ADHD patients against the healthy controls.

The MX-FAR model produced novel and interesting findings in the analysis of the ADHD EEG data. Using the central channel Cz as a reference signal, the MX-FAR model was able to identify more pronounced non-linear dependence structures for the ADHD

group. This is a novel finding from this dataset. When the reference signal exhibits large amplitudes, the MX-FAR model captures more inter-channel directional links in the brain network of the ADHD population. This non-linear connectivity among ADHD individuals may be associated with their shorter attention span. Similarly, non-linearity is observed when an ADHD patient is either at rest or performing a task as a result of cortical dysfunctions in the neuropsychiatric disorder Sohn et al. (2010). On the other hand, subjects in the healthy control group seem to have more consistent (linear) cross-channel dependence. That is, for the entire duration of the experiment, information flow from a channel to another works continuously, regardless of the amplitudes in the reference signal. Lastly, we see that information from the visual processing channels are more optimized and channels in regions with similar cognitive functions have better connection for individuals without the disorder.

Finally, even though the proposed model is here applied to EEG signals, the modeling framework is very general and may have potential applications in entirely different contexts. For example, Gross Domestic Product (GDP) from different countries may be explained through the MX-FAR model, where GDPs from top producing countries may serve as the reference signals as they drive the global economy. The same model may be useful for stock market prices where leading companies dictate the direction of the market.

References

- Alchalabi, A. E., Shirmohammadi, S., Eddin, A. N. & Elsharnouby, M. (2018), ‘Focus: detecting ADHD patients by an EEG-based serious game’, IEEE Transactions on Instrumentation and Measurement **67**(7), 1512–1520.
- Arns, M., Conners, C. K. & Kraemer, H. C. (2013), ‘A decade of EEG theta/beta ratio research in ADHD: a meta-analysis’, Journal of Attention Disorders **17**(5), 374–383.
- Baccalá, L. A. & Sameshima, K. (2001), ‘Partial directed coherence: a new concept in neural structure determination’, Biological Cybernetics **84**(6), 463–474.
- Barry, R. J., Clarke, A. R., McCarthy, R. & Selikowitz, M. (2002), ‘EEG coherence in attention-deficit/hyperactivity disorder: a comparative study of two DSM-IV types’, Clinical Neurophysiology **113**(4), 579–585.
- Bigdely-Shamlo, N., Mullen, T., Kothe, C., Su, K.-M. & Robbins, K. A. (2015), ‘The PREP pipeline: standardized preprocessing for large-scale EEG analysis’, Frontiers in Neuroinformatics **9**, 16.
- Bjørge, L.-E. N. & Emaus, T. H. (2017), Identification of EEG-based signature produced by visual exposure to the primary colors RGB, Master’s thesis, Norwegian University of Science and Technology.
- Brockwell, P. J. & Davis, R. A. (2009), Time Series: Theory and Methods, Springer Science & Business Media.
- Brown, M. R., Sidhu, G. S., Greiner, R., Asgarian, N., Bastani, M., Silverstone, P. H., Greenshaw, A. J. & Dursun, S. M. (2012), ‘ADHD-200 global competition: diagnosing ADHD using personal characteristic data can outperform resting state fMRI measurements’, Frontiers in Systems Neuroscience **6**, 69.
- Cai, Z., Fan, J. & Yao, Q. (2000), ‘Functional-coefficient regression models for nonlinear time series’, Journal of the American Statistical Association **95**(451), 941–956.
- Chen, H., Song, Y. & Li, X. (2019), ‘A deep learning framework for identifying children with ADHD using an EEG-based brain network’, Neurocomputing **356**, 83–96.

- Chen, R. & Liu, L.-M. (2001), ‘Functional coefficient autoregressive models: estimation and tests of hypotheses’, Journal of Time Series Analysis **22**(2), 151–173.
- Chen, R. & Tsay, R. S. (1993), ‘Functional-coefficient autoregressive models’, Journal of the American Statistical Association **88**(421), 298–308.
- Cimenser, A., Purdon, P. L., Pierce, E. T., Walsh, J. L., Salazar-Gomez, A. F., Harrell, P. G., Tavares-Stoeckel, C., Habeeb, K. & Brown, E. N. (2011), ‘Tracking brain states under general anesthesia by using global coherence analysis’, Proceedings of the National Academy of Sciences **108**(21), 8832–8837.
- Clarke, A. R., Barry, R. J., McCarthy, R., Selikowitz, M., Johnstone, S. J., Hsu, C.-I., Magee, C. A., Lawrence, C. A. & Croft, R. J. (2007), ‘Coherence in children with attention-deficit/hyperactivity disorder and excess beta activity in their EEG’, Clinical Neurophysiology **118**(7), 1472–1479.
- Cortese, S., Kelly, C., Chabernaud, C., Proal, E., Di Martino, A., Milham, M. P. & Castellanos, F. X. (2012), ‘Toward systems neuroscience of ADHD: a meta-analysis of 55 fMRI studies’, American Journal of Psychiatry **169**(10), 1038–1055.
- Erkuş, E. C. (2017), Graph theory analyses on connectivity maps obtained by partial directed coherence using EEG data of dyslexic and healthy children, Master’s thesis, Middle East Technical University.
- Gorrostieta, C., Ombao, H., Bédard, P. & Sanes, J. N. (2012), ‘Investigating brain connectivity using mixed effects vector autoregressive models’, NeuroImage **59**(4), 3347–3355.
- Gualtieri, C. T. & Johnson, L. G. (2005), ‘ADHD: Is objective diagnosis possible?’, Psychiatry (Edgmont) **2**(11), 44.
- Harvill, J. L. & Ray, B. K. (2006), ‘Functional coefficient autoregressive models for vector time series’, Computational Statistics & Data Analysis **50**(12), 3547–3566.
- Henderson, C. R. (1953), ‘Estimation of variance and covariance components’, Biometrics **9**(2), 226–252.
- Huang, J. Z. & Shen, H. (2004), ‘Functional coefficient regression models for non-linear time series: a polynomial spline approach’, Scandinavian Journal of Statistics **31**(4), 515–534.

- Jasper, H. H., Solomon, P. & Bradley, C. (1938), ‘Electroencephalographic analyses of behavior problem children’, American Journal of Psychiatry **95**(3), 641–658.
- Jiang, K., Yi, Y., Li, L., Li, H., Shen, H., Zhao, F., Xu, Y. & Zheng, A. (2019), ‘Functional network connectivity changes in children with attention-deficit hyperactivity disorder: a resting-state fMRI study’, International Journal of Developmental Neuroscience **78**, 1–6.
- Lenartowicz, A. & Loo, S. K. (2014), ‘Use of EEG to diagnose ADHD’, Current Psychiatry Reports **16**(11), 498.
- Mohammadi, M. R., Khaleghi, A., Nasrabadi, A. M., Rafieivand, S., Begol, M. & Zarafshan, H. (2016), ‘EEG classification of ADHD and normal children using non-linear features and neural network’, Biomedical Engineering Letters **6**(2), 66–73.
- Motie Nasrabadi, A., Allahverdy, A., Samavati, M. & Mohammadi, M. R. (2020), ‘EEG data for ADHD / control children’.
URL: <https://dx.doi.org/10.21227/rzjfh-zn36>
- Murias, M., Swanson, J. M. & Srinivasan, R. (2007), ‘Functional connectivity of frontal cortex in healthy and ADHD children reflected in EEG coherence’, Cerebral Cortex **17**(8), 1788–1799.
- Muthuraman, M., Moliadze, V., Boecher, L., Siemann, J., Freitag, C. M., Groppa, S. & Siniatchkin, M. (2019), ‘Multimodal alterations of directed connectivity profiles in patients with attention-deficit/hyperactivity disorders’, Scientific Reports **9**(1), 1–13.
- Nunez, M. D., Nunez, P. L., Srinivasan, R., Ombao, H., Linnquist, M., Thompson, W. & Aston, J. (2016), ‘Electroencephalography (EEG): neurophysics, experimental methods, and signal processing’, Handbook of Neuroimaging Data Analysis pp. 175–197.
- Nunez, P. L., Srinivasan, R. et al. (2006), Electric fields of the brain: the neurophysics of EEG, Oxford University Press, USA.
- Ombao, H., Von Sachs, R. & Guo, W. (2005), ‘Slex analysis of multivariate nonstationary time series’, Journal of the American Statistical Association **100**(470), 519–531.
- Schelter, B., Winterhalder, M., Eichler, M., Peifer, M., Hellwig, B., Guschlbauer, B., Lücking, C. H., Dahlhaus, R. & Timmer, J. (2006), ‘Testing for directed influences

- among neural signals using partial directed coherence', Journal of Neuroscience Methods **152**(1-2), 210–219.
- Shumway, R. H., Stoffer, D. S. & Stoffer, D. S. (2000), Time series analysis and its applications, Vol. 3, Springer.
- Sobanski, E. (2006), 'Psychiatric comorbidity in adults with attention-deficit/hyperactivity disorder (ADHD)', European Archives of Psychiatry and Clinical Neuroscience **256**(1), i26–i31.
- Sohn, H., Kim, I., Lee, W., Peterson, B. S., Hong, H., Chae, J.-H., Hong, S. & Jeong, J. (2010), 'Linear and non-linear EEG analysis of adolescents with attention-deficit/hyperactivity disorder during a cognitive task', Clinical Neurophysiology **121**(11), 1863–1870.
- Swartwood, J. N., Swartwood, M. O., Lubar, J. F. & Timmermann, D. L. (2003), 'EEG differences in ADHD-combined type during baseline and cognitive tasks', Pediatric Neurology **28**(3), 199–204.
- Tcheslavski, G. V. & Beex, A. L. (2006), 'Phase synchrony and coherence analyses of EEG as tools to discriminate between children with and without attention deficit disorder', Biomedical Signal Processing and Control **1**(2), 151–161.
- van Dijk, H., deBeus, R., Kerson, C., Roley-Roberts, M. E., Monastra, V. J., Arnold, L. E., Pan, X. & Arns, M. (2020), 'Different spectral analysis methods for the theta/beta ratio calculate different ratios but do not distinguish ADHD from controls', Applied Psychophysiology and Biofeedback **45**, 165–173.